Dynamics and Adaptive Control of a Novel 5D Hyperchaotic System: Either Hidden Attractor or Self-excited with Unusual Nature of Unstable Equilibria

Sagban, L. J.[1] and Shukur, A. A.[*1]

[1]*Department of Mathematics, Faculty of Computer Science and Mathematics,
University of Kufa, Iraq*

E-mail: shukur.math@gmail.com
Corresponding author

Abstract

In 2020, J. Sprott proposed a new three dimensional chaotic system with special features such like 1) dissipative and time-reversible; 2) no equilibrium point; 3) lien of initial conditions goes to the attractor. We observed that an extension of the so-called Sprott's 2020 system to four dimensional system with complex dynamics showed either chaotic or hyperchaotic with unbounded orbits. In this paper, a novel five dimensional hyperchaotic system based on Sprott's 2020 system has been proposed. The proposed system shows complex dynamics like hyperchaotic. The proposed system can be classified as a hidden attractor where no equilibrium point appeared or self-excited where an unusual nature of unstable equilibrium points connected to a very complicated function called Lambert W appeared. The dynamical properties of such system are discovered by computing the Lyapunov exponents and bifurcation diagram. Adaptive control to the proposed system was provided.

Keywords: hyperchaotic system; hidden attractor; equilibrium point; Lambert W function.

1   Introduction

Chaos phenomena motivated researchers to propose a large number of chaotic systems during the last two decades. Chaos is an applicable object almost everywhere, such as in weather forecasting [23], telecommunication [26, 2], vibration control systems [8], biological modeling [21] and others. During the last decades, researchers attempted to obtain a chaotic systems with special characteristics such as the type of the equilibrium points, the following special systems were extra cited after the first system introduced after Lorenz's system (in [13]):

- Wei's system which has no equilibria, see [30].

- Wang's system which has only one stable equilibrium, see [33].

- Jafari and Sprott considered a chaotic system with line equilibrium, see [9]. Another example of chaotic system with line equilibrium was obtained in [20].

- Wang's system with saddle-focus equilibrium, see [29].

- Jafari et al. considered a chaotic system with surfaces of equilibria, see [10].

Chaotic systems with more than one positive Lyapunov exponent were first indicated by Rössler in the late 1970s, which were called hyperchaotic [18]. In cases of hyperchaotic behavior, the Shilnikov approach may not be helpful in verifying the chaos of such systems due to their unique features, as they cannot have either a homoclinic or heteroclinic orbit. Thus, hyperchaotic systems are more complicated. Later, the investigations of hyperchaotic systems rapidly grew, and their application appeared in different areas, especially secure communications due to their high complexity, which shows no possibility to retrieve hidden messages. For instance, Ammar et al. [14] proposed a 3-dimensional hyperbolic function conservative chaotic system and selected two sequences generated by this system, which are combined with a self-invertible matrix for color image encryption. Khan et al. in [11] proposed a hyperbolic memristor based 6-dimensional chaotic model for encryption. A square image encrypted by using a symmetrical high four dimensional hyperchaotic system with two exponential functions in [22]. An unusual complicated chaotic system was proposed in [19] with an image encryption application. Comparing with different methods of image encryption like [15], image encryption based on hyperchaotic systems is very successful.

A new method of communication encryption involved to 6-dimensional hyperchaotic Lorenz system with circuit simulation to verify the security of the communication scheme was described in [32]. A 6-dimensional hyperchaotic system was applied to complete the signal encryption and decryption circuit design of a secure communication scheme in [6]. A secure communication based on a microcontroller corresponds to a new 5-dimensional hyperchaotic system [28]. A memristive cellular neural network hyperchaotic system and a new 5-dimensional memristive hyperchaotic system based on hyperchaotic Lu system were presented in [16, 31], respectively. A new 5-dimensional hyperchaotic system with three equilibrium points and deduce that the new hyperchaotic system has three positive Lyapunov exponents was proposed in [5].

On the other hand, the literature suggests that one of the earliest control strategies for resolving the synchronization issue was the active control strategy. In this regard, Bai and Lonngren in [3, 4] showed that active control theory may synchronize connected Lorenz systems. At the simulation level, the synchronization was confirmed. A control strength matrix was added to the active control by Tang et al. [25], where they demonstrated that it is easier to accomplish total synchronization of chaos using this enhanced strategy. The latter was verified by numerical simulations

on the Rössler, Liu's four-scroll, and Chen systems. Furthermore, Yassen [34] reported on the synchronizations between two distinct chaotic systems, namely the Lorenz and Lu systems, Chen and Lu system, and Lorenz and Chen systems. However, Perez-Cruz et al. [17] looked into the synchronization of a new three-dimensional chaotic system by using Lyapunov analysis to design a nonlinear controller that guaranteed the synchronization error's exponential convergence, and the outcomes of their numerical simulation confirmed the controller's excellent performance. In [27], Varan and Akful used a Lyapunov function to synchronize a hyperchaotic system and attain global asymptotic stability. The efficacy of the suggested active control approach was verified using numerical analysis. Finally, Zhu and Du in [35] used active control to solve the anti-synchronization of systems, and numerical simulations were used to confirm the control's viability. Recently, anti-synchronization of a novel 5-dimensional hyperchaotic system was investigated in [1].

Besides, the phenomenon of hidden attractor has a very rapid rate of investigation where the basin of attraction does not contain neighbourhoods of the equilibrium points and has been investigated by a large number of researchers. Kuznetsov et al. in [12] provided a simulation of hidden attractors in dynamical systems. Such examples of hidden attractors are chaotic systems without equilibrium points.

This paper is organized as follows: in Section 2, we propose a novel 5-dimensional hyperchaotic system with five non-linear terms and five linear terms. In Section 3, system analysis such as stability, dissipativity, and the Kaplan Yorke dimension were investigated. In Section 4, the possibility of the synchronization scheme of the proposed systems was studied.

2   The Proposed System

Sprott in [24] posed a crucial question regarding the need for additional examples of chaos: "Do we need more chaos examples?" In response to this question, Sprott provided a positive answer by introducing a new three dimensional chaotic system:

$$\begin{cases} \dot{x} = y, \\ \dot{y} = -x - sgn(z)y, \\ \dot{z} = y^2 - e^{-x^2}. \end{cases} \tag{1}$$

System (1) has the following characteristics: 1) dissipative and time-reversible; 2) has no equilibria; 3) has multifractal attractor that is hidden but whose basin includes the whole of the three-dimensional space so it has a lien of initial conditions goes to the attractor; 4) has initial conditions seem to point toward the attractor, which has a capacity dimension of 3 and fills all of space with a very nonuniform measure.

Observation. Given the importance of hyperchaotic systems, we attempted to extend Sprott's 3-dimensional system to a 4-dimensional version. However, all our attempts resulted in systems that were either chaotic or hyperchaotic but had unbounded orbits, which we found to be less interesting.

L. J. Sagban and A. A. Shukur

Malaysian J. Math. Sci. 18(3): 675–696 (2024) *675 - 696*

Based on Sprott's system, we propose the following five dimensional hyperchaotic:

$$\begin{cases} \dot{x} = y - \alpha w sgn(z) - \sigma u, \\ \dot{y} = -x - zy, \\ \dot{z} = y^2 - e^{-x^2} - \beta, \\ \dot{w} = \gamma x - \nu y, \\ \dot{u} = \xi + \sin(z), \end{cases} \quad (2)$$

where $\alpha, \beta, \gamma, \nu, \xi, \sigma$ are system's parameter and x, y, z, w, u are system variables.

2.1 Dynamical analysis

In what follows, we test the most important peculiarities of complex dynamical systems such as stability, dissipativity, Lyapunov exponents (LEs) and bifurcation diagram.

2.2 Symmetry

System (2) possesses the invariance with the coordinate transformation,

$$(x, y, z, w, u) \to (-x, -y, z, -w, -u).$$

The system (2) is symmetrical about the coordinate axis z.

2.3 Stability

To set the stability and have a better understanding of the nature of the appeared equilibrium points, we will provide a brief introduction into the Lambert W function. The following equation has an infinity countable number of solutions:

$$se^s = z,$$

where z is a complex number. For integers k represented by $W_k(z)$. A Lambert W function branches are:

1. When $k = 0$, the branches called the principal branch.

2. When $k = -1$, every branch excludes the real axis has range of $W_1(z)$ includes $(-\infty, -1/e]$.

Note that only $W_0(z)$ has positive values range, see Figure 1. When $z = -1/e$, there exists a double root $s = -1$ of the basic equation $se^s = z$. The typical branch selection process assigns

$$W_0(-1/e) = W_{-1}(-1/e) = -1.$$

Each branch is an analytic complex function. The Lambert W function has a very special graphic and complicated structure, see [7].

L. J. Sagban and A. A. Shukur

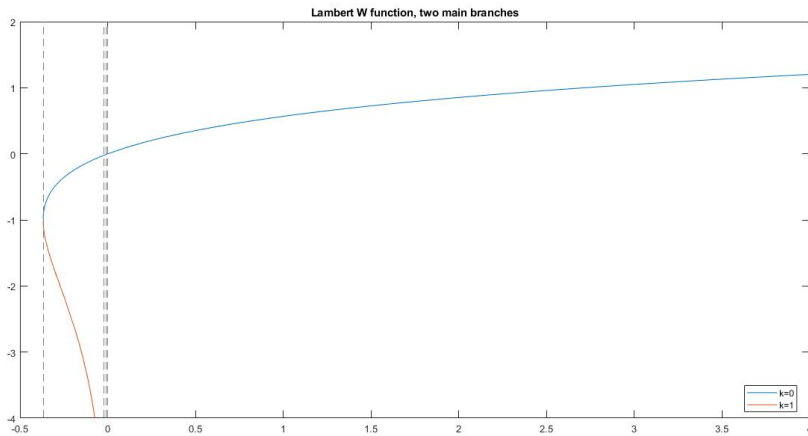*Malaysian J. Math. Sci.* 18(3): *675–696* (2024) *675 - 696*

Figure 1: The graph of Lambert W function.

Next, to show the stability of system (2), the following algebraic equations must be held:

$$y - \alpha w sgn(z) - \sigma u = 0, \tag{3}$$

$$-x - yz = 0, \tag{4}$$

$$y^2 - e^{-x^2} - \beta = 0, \tag{5}$$

$$\gamma x - \nu y = 0, \tag{6}$$

$$\xi + \sin(z) = 0. \tag{7}$$

Solving the equations in (3)-(7) shows the following two cases:

1. If $\xi = 0$ in (7), then it follows that the systems (2) has no equilibrium point. In this case, attractors generated by system (2) are hidden strange attractors.

2. From (6) follows that $x = \frac{\nu}{\gamma} y$. By substituting the value of x in (5), we obtain that

$$y = \frac{1}{\nu} \sqrt{\gamma^2 W \left(\frac{\nu^2 \exp \left[\frac{\beta \nu^2}{\gamma^2} \right]}{\gamma^2} \right) + \beta \nu^2},$$

and

$$x = \frac{1}{\gamma} \sqrt{\gamma^2 W \left(\frac{\nu^2 \exp \left[\frac{\beta \nu^2}{\gamma^2} \right]}{\gamma^2} \right) + \beta \nu^2}.$$

Again by substituting the values of x and y in (4), we obtain that $z = \frac{-\nu}{\gamma}$. Obviously, if $w = 0$ and

$$u = \frac{1}{\sigma\nu}\sqrt{\gamma^2 W\left(\frac{\nu^2 \exp\left[\frac{\beta\nu^2}{\gamma^2}\right]}{\gamma^2}\right) + \beta\nu^2},$$

then the Equation (3) is equal to zero. Now, if $\xi = \sin\left(\frac{-\nu}{\gamma}\right)$ in (7), then a very complicated nature of equilibrium points appeared and it is related to so-called Lambert W function, such as:

$$S_{1,1} = \begin{cases} \frac{1}{\gamma}\sqrt{\gamma^2 W\left(\frac{\nu^2 \exp\left[\frac{\beta\nu^2}{\gamma^2}\right]}{\gamma^2}\right) + \beta\nu^2}, \\[2ex] \frac{1}{\nu}\sqrt{\gamma^2 W\left(\frac{\nu^2 \exp\left[\frac{\beta\nu^2}{\gamma^2}\right]}{\gamma^2}\right) + \beta\nu^2}, \\[2ex] \frac{-\nu}{\gamma}, \\[1ex] 0, \\[1ex] \frac{1}{\sigma\nu}\sqrt{\gamma^2 W\left(\frac{\nu^2 \exp\left[\frac{\beta\nu^2}{\gamma^2}\right]}{\gamma^2}\right) + \beta\nu^2}, \end{cases}$$

and

$$S_{1,2} = \begin{cases} \frac{-1}{\gamma}\sqrt{\gamma^2 W\left(\frac{\nu^2 \exp\left[\frac{\beta\nu^2}{\gamma^2}\right]}{\gamma^2}\right) + \beta\nu^2}, \\[2ex] \frac{-1}{\nu}\sqrt{\gamma^2 W\left(\frac{\nu^2 \exp\left[\frac{\beta\nu^2}{\gamma^2}\right]}{\gamma^2}\right) + \beta\nu^2}, \\[2ex] \frac{-\nu}{\gamma}, \\[1ex] 0, \\[1ex] \frac{-1}{\sigma\nu}\sqrt{\gamma^2 W\left(\frac{\nu^2 \exp\left[\frac{\beta\nu^2}{\gamma^2}\right]}{\gamma^2}\right) + \beta\nu^2}, \end{cases}$$

where $W(.)$ is a Lambert W function.

This obviously shows that the equilibrium points of (2) has a complicated nature, for instance, the stability depends on the value of $\beta, \gamma, \nu, \sigma$ under the action of the mentioned function. In particular, setting the stability of the system (2) is possible by calculating the Jacobian matrices at the possible equilibrium points:

$$J_0 = \begin{pmatrix} 0 & 1 & -2\alpha w\, dirac(z) & -\alpha sgn(z) & -\sigma \\ -1 & -z & -y & 0 & 0 \\ 2xe^{-x^2} & 2y & 0 & 0 & 0 \\ \gamma & -\nu & 0 & 0 & 0 \\ 0 & 0 & \cos(z) & 0 & 0 \end{pmatrix}, \tag{8}$$

where $dirc(z)$ is the Dirac function. The corresponding characteristic polynomial of $J_{S_{1,1};S_{1,2}}$ is

$$P(\lambda) = \lambda^5 + a_4\lambda^4 + a_3\lambda^3 + a_2\lambda^2 + a_1\lambda_1, \tag{9}$$

where

$$\begin{cases} a_5 = -1, \\ a_4 = 1, \\ a_3 = \alpha\gamma - 2J^2 - 1, \\ a_2 = \alpha\nu - \alpha\gamma - JK - \sigma\cos\left(\frac{\nu}{\gamma}\right)K, \\ a_1 = 2\alpha\nu J^2 - \alpha\nu jK + 2\sigma\cos\left(\frac{\nu}{\gamma}\right)J + \sigma\cos\left(\frac{\nu}{\gamma}\right)K, \end{cases} \tag{10}$$

$$J = \frac{1}{\gamma}\sqrt{\gamma^2 W\left(\frac{\nu^2\exp\left[\frac{\beta\nu^2}{\gamma^2}\right]}{\gamma^2}\right) + \beta\nu^2},$$

and

$$K = \frac{2}{\nu}\sqrt{\gamma^2 W\left(\frac{\nu^2\exp\left[\frac{\beta\nu^2}{\gamma^2}\right]}{\gamma^2}\right) + \beta\nu^2}\left(\exp\left[-\frac{\gamma^2 W\left(\frac{\nu^2\exp\left[\frac{\beta\nu^2}{\gamma^2}\right]}{\gamma^2}\right) + \beta\nu^2}{\nu^2}\right]\right).$$

In both above cases, system (2) shows a complex dynamics such hperchaotic behavior indicates when the initial condition is $x_0, y_0, z_0, w_0, u_0 = (1,1,1,1,1)$ and $\alpha = 1.5, \beta = 30.9, \gamma = 3.5$, $\nu = 0.2, \sigma = 0.5, \xi = \sin\left(\frac{-0.2}{3.5}\right) = -0.0571118$. In the following, we calculate the eigenvalues of the second case for those parameters. The eigenvalues are

$$\begin{cases} \lambda_{1,2} &= \pm 2.3405, \\ \lambda_{3,4} &= 0.0208 \pm 3.2166i, \\ \lambda_5 &= 0. \end{cases} \tag{11}$$

Due to the Routh-Hurwitz stability criterion and (11), obviously the system (2) has two unstable saddle-focus node points.

2.4 The Kaplan Yorke fractional dimension

The Kaplan Yorke fractional dimension, which presents the complexity of the attractor, is defined by

$$D_{KY} = j + \frac{\sum_{i=1}^{j} L_i}{|L_{j+1}|}, \tag{12}$$

where j is the largest integer satisfying $\sum_{i=1}^{j} L_i \geq 0$ and $\sum_{i=1}^{j+1} L_i < 0$. The LEs and the Kaplan Yorke fractional dimension of system (2) for $\xi = 0$ or $\xi = -0.0571118$ with fixing $\alpha = 1.5$, $\beta = 30.9, \gamma = 3.5, \nu = 0.2, \sigma = 0.5$ are shown in Table 1 (see Figure 2).

Table 1: LEs and D_{YK} of system (2).

The values of ξ	LEs	D_{KY}
$\xi = 0$	$L_1 = 0.48938$	4.832
	$L_2 = 0.19982$	
	$L_3 = 0$	
	$L_4 = -0.18097$	
	$L_5 = -0.61035$	
$\xi = -0.0571118$	$L_1 = 0.55705$	4.854
	$L_2 = 0.23368$	
	$L_3 = 0$	
	$L_4 = -0.19908$	
	$L_5 = -0.69207$	
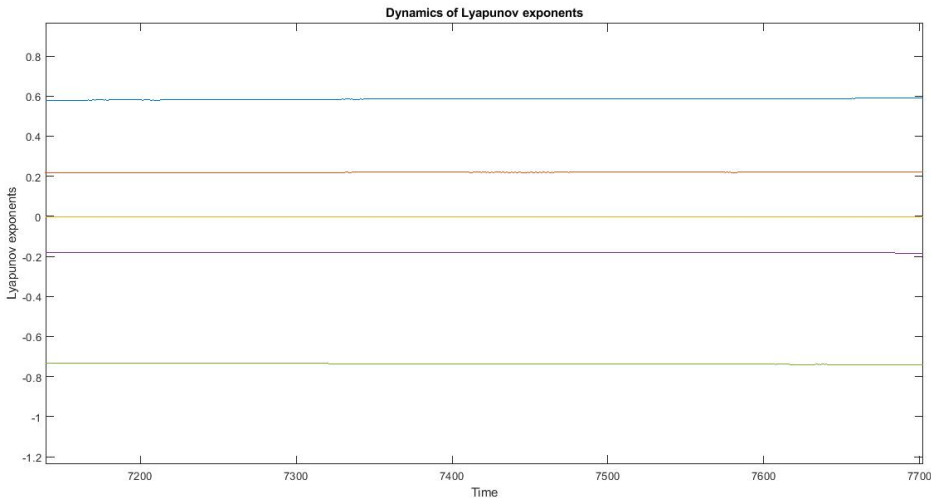
Figure 2: The Lyapunov exponents of the system (2) when $\xi = 0$.

2.5 Dissipativity

The dissipativity of system (2) shows

$$V = \frac{\partial \dot{x}}{\partial x} + \frac{\partial \dot{y}}{\partial y} + \frac{\partial \dot{z}}{\partial z} + \frac{\partial \dot{w}}{\partial w} + \frac{\partial \dot{u}}{\partial u} = -z. \tag{13}$$

Obviously, Sines, the dissipativity of the trajectory of (2) due to the dissipation is shown by the time-averaged value $-z(t)$. In [29] was established the average value of any function of time $q(t)$ which is

$$\overline{q}(t) = \lim_{t \to \infty} \left(\int_{t_0}^{t} q(t)qt/t - t_0 \right). \tag{14}$$

Now, one can verify that the average of $z(t)$ of system (2) is grater than zero. This can be seen in Figure 3. So, (2) is dissipative. Moreover, in Figures 4 - 6, the bifurcation diagrams for varied values of α, β, ξ are shown. The phase portraits of the proposed system (2) is presented in Figure 7.

L. J. Sagban and A. A. Shukur

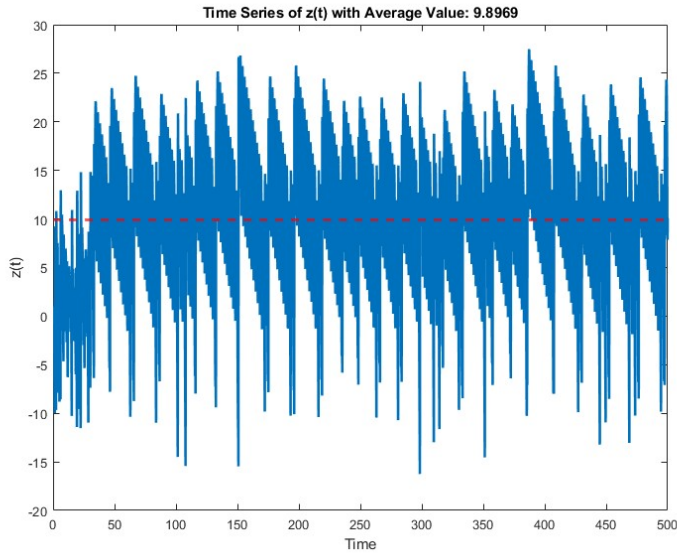*Malaysian J. Math. Sci.* 18(3): 675–696 (2024) *675 - 696*

Figure 3: Average value of $z(t)$ of the system (2).

Observation 2. Other notable remark we observed is that the system (2) preserves the features of the original system Sprott's system when $\xi = 0$ while only II and III properties of Sprott's system were preserved when $\xi = -0.0571118$.
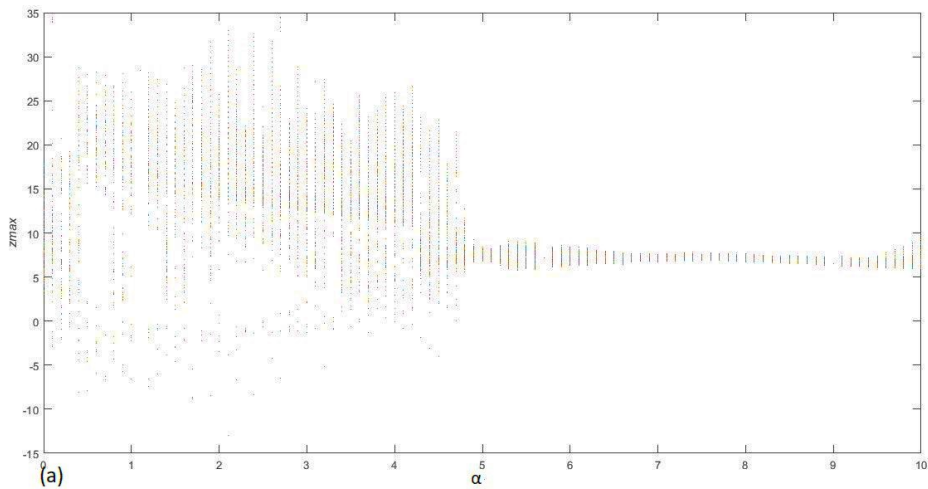

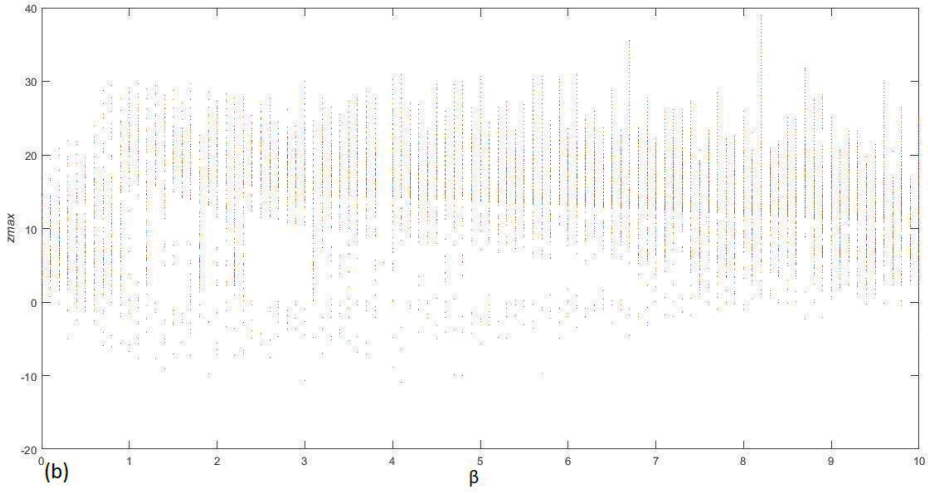
Figure 4: Bifurcation diagram of system (2) when varying α.

L. J. Sagban and A. A. Shukur

Malaysian J. Math. Sci. 18(3): 675–696 (2024) *675 - 696*

Figure 5: Bifurcation diagram of system (2) when varying β.
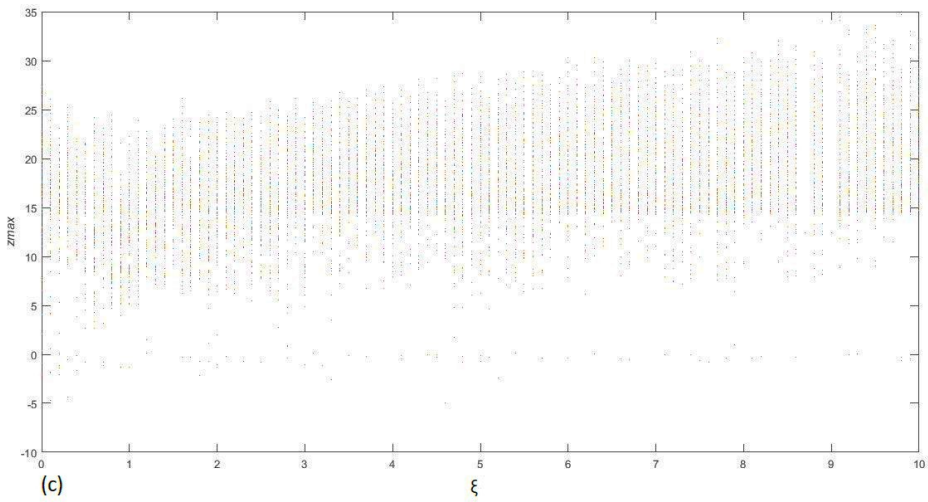
Figure 6: Bifurcation diagram of system (2) when varying ξ.

L. J. Sagban and A. A. Shukur

Malaysian J. Math. Sci. 18(3): 675–696 (2024) *675 - 696*
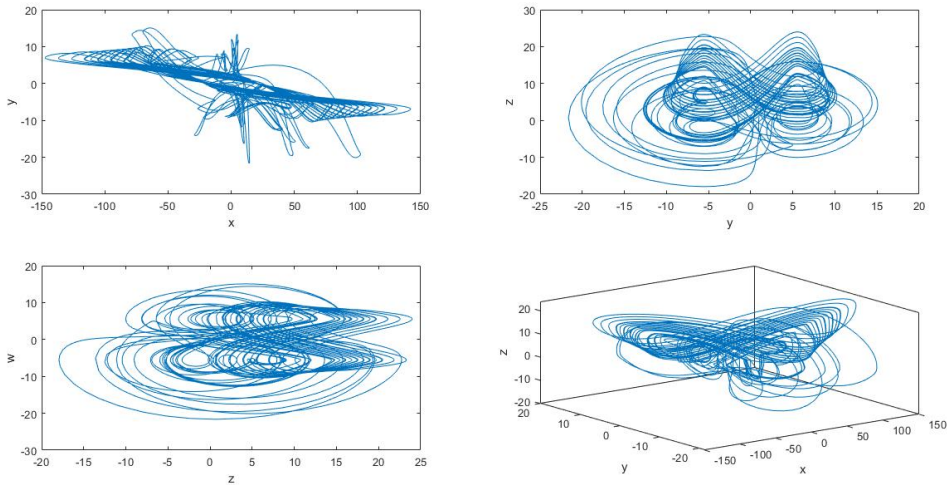
Figure 7: The phase plane of system (2) when $\xi = 0$.

3 Coexisting Attractors

In order to study the phenomenon of coexisting attractors, we must first determine how the parameters and initial conditions affect the system's behavior (2).

For high-dimensional (dim > 3) hyperchaotic systems, its not surprising if the system shows chaotic behavior or periodic orbit. For instance, when the initial condition are given by $(x_0, y_0, z_0, w_0) = (1, 1, 1, 1)$, the system (2) reveals chaotic dynamics if $\beta = \xi = 0$ where LEs are: $L_1 = 0.09785, L_2 = 0, L_3 = -0.00831, L_4 = -0.11429, L_5 = -0.27701$ (see Figure 8) or displays a coexisting of periodic orbit if $\alpha = 2, \beta = \xi = 0, \gamma = \nu = 1$.
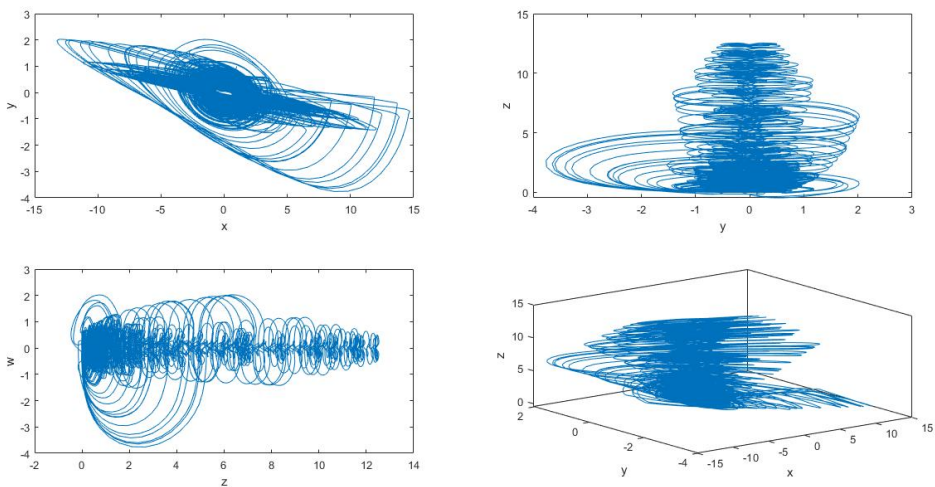

Figure 8: The phase plane of system (2) when $\beta = \xi = 0$.

4   Adaptive Control of the Proposed Chaotic System

Let define the driver system by

$$
\begin{cases}
\dot{x_1} = x_2 - \alpha x_4 sgn(x_3) - \sigma x_5, \\
\dot{x_2} = -x_1 - x_2 x_3, \\
\dot{x_3} = x_2^2 - e^{-x_1^2} - \beta, \\
\dot{x_4} = \gamma x_1 - \nu x_2, \\
\dot{x_5} = \xi + \sin x_3.
\end{cases}
\tag{15}
$$

In what follow, we provide the adaptive synchronization of identical novel hyperchaotic system with parameters which are not valued. The response system is presented as

$$
\begin{cases}
\dot{x_1} = x_2 - \alpha x_4 sgn(x_3) - \sigma x_5 + u_1, \\
\dot{x_2} = -x_1 - x_2 x_3 + u_2, \\
\dot{x_3} = x_2^2 - e^{-x_1^2} - \beta + u_3, \\
\dot{x_4} = \gamma x_1 - \nu x_2 + u_4, \\
\dot{x_5} = \xi + \sin x_3 + u_5,
\end{cases}
\tag{16}
$$

where x_1, x_2, x_3, x_4, x_5 are the states, $\alpha, \beta, \gamma, \nu, \sigma, \xi$ are unknown system parameters and

$$
U = [u_1, u_2, u_3, u_4, u_5]^T,
$$

is the adaptive controller to be determined. We consider the adaptive controller defined by

$$
\begin{cases}
u_1 = -x_2 + \varepsilon_\alpha(t) x_4 sgn(x_3) + \varepsilon_\sigma(t) x_5 - k_1 x_1, \\
u_2 = x_1 + x_2 x_3 - k_2 x_2, \\
u_3 = -x_2^2 + e^{-x_1^2} + \varepsilon_\beta(t) - k_3 x_3, \\
u_4 = -\varepsilon_\gamma(t) x_1 + \varepsilon_\nu(t) x_2 - k_4 x_4, \\
u_5 = -\varepsilon_\xi(t) - \sin(t) x_3 - k_5 x_5,
\end{cases}
\tag{17}
$$

where $\varepsilon_\alpha, \varepsilon_\beta, \varepsilon_m, \varepsilon_d, \varepsilon_r$ denote the estimated parameters of the system coefficients α, β, m, d, r respectively and $k_1, k_2, k_3, k_4, k_5 > 0$. By substituting (17) into (16), we obtain the closed-loop system:

$$
\begin{cases}
\dot{x_1} = -[\alpha - \varepsilon_\alpha(t)] x_4 sgn(x_3) - [\sigma - \varepsilon_\sigma(t)] x_5 - k_1 x_1, \\
\dot{x_2} = -k_2 x_2, \\
\dot{x_3} = -[\beta - \varepsilon_\beta(t)] - k_3 x_3, \\
\dot{x_4} = [\gamma - \varepsilon_\gamma(t)] x_1 - [\nu - \varepsilon_\nu(t)] x_2 - k_4 x_4, \\
\dot{x_5} = [\xi - \varepsilon_\xi(t)] - k_5 x_5.
\end{cases}
\tag{18}
$$

Accordingly, let us denote the error estimation of the parameters as follows:

$$
\begin{cases}
\varepsilon_1(t) = [\alpha - \varepsilon_\alpha(t)], \\
\varepsilon_2(t) = [\beta - \varepsilon_\beta(t)], \\
\varepsilon_3(t) = [\gamma - \varepsilon_\gamma(t)], \\
\varepsilon_4(t) = [\nu - \varepsilon_\nu(t)], \\
\varepsilon_5(t) = [\xi - \varepsilon_\xi(t)], \\
\varepsilon_6(t) = [\sigma - \varepsilon_\sigma(t)].
\end{cases}
\tag{19}
$$

L. J. Sagban and A. A. Shukur

Malaysian J. Math. Sci. 18(3): 675–696 (2024) 675 - 696

Based on Equation (19), the derivatives of parameter estimation errors can be expressed as:

$$
\begin{cases}
\dot{\varepsilon_1} = -\dot{\varepsilon_\alpha}, \\
\dot{\varepsilon_2} = -\dot{\varepsilon_\beta}, \\
\dot{\varepsilon_3} = -\dot{\varepsilon_\gamma}, \\
\dot{\varepsilon_4} = -\dot{\varepsilon_\nu}, \\
\dot{\varepsilon_5} = -\dot{\varepsilon_\sigma}.
\end{cases}
\tag{20}
$$

Next, we reduce (18) to

$$
\begin{cases}
\dot{x_1} = -\varepsilon_1 x_4 sgn(x_3) - \varepsilon_6 x_5 - k_1 x_1, \\
\dot{x_2} = -k_2 x_2, \\
\dot{x_3} = -\varepsilon_2 - k_3 x_3, \\
\dot{x_4} = \varepsilon_3 x_1 - \varepsilon_4 x_2 - k_4 x_4, \\
\dot{x_5} = \varepsilon_5 - k_5 x_5.
\end{cases}
\tag{21}
$$

Theorem 4.1. *If the controller are chosen as* (17) *and let the parameter's update laws is*

$$
\begin{cases}
\dot{\varepsilon_1}(t) = x_1 x_4 sgn(x_3) - \eta(\alpha - \varepsilon_\alpha), \\
\dot{\varepsilon_2}(t) = x_3 - \eta(\beta - \varepsilon_\beta), \\
\dot{\varepsilon_3}(t) = -x_1 x_4 - \eta(\gamma - \varepsilon_\gamma), \\
\dot{\varepsilon_4}(t) = x_2 x_4 - \eta(\nu - \varepsilon_\nu), \\
\dot{\varepsilon_5}(t) = x_5 - \eta(\xi - \varepsilon_\xi), \\
\dot{\varepsilon_6}(t) = x_1 x_5 - \eta(\sigma - \varepsilon_\sigma).
\end{cases}
\tag{22}
$$

Then, the synchronization between the driver system (17) *and the response system* (16) *is approached if* k_1, k_2, k_3, k_4, k_5 *are positive constants.*

Proof. We consider the Lyapunov function defined by

$$
V(x_1, x_2, x_3, x_4, x_5, \varepsilon_1, \varepsilon_2, \varepsilon_3, \varepsilon_4, \varepsilon_5, \varepsilon_6) = \frac{1}{2} \left(x_1^2 + x_2^2 + x_3^2 + x_4^2 + x_5^2 + \varepsilon_1^2 + \varepsilon_2^2 + \varepsilon_3^2 + \varepsilon_4^2 + \varepsilon_5^2 + \varepsilon_6^2 \right).
$$

Differentiating the above function, we have

$$
\dot{V}(x_1, x_2, x_3, x_4, x_5, \varepsilon_1, \varepsilon_2, \varepsilon_3, \varepsilon_4, \varepsilon_5, \varepsilon_6) =
$$
$$
(x_1 \dot{x_1} + x_2 \dot{x_2} + x_3 \dot{x_3} + x_4 \dot{x_4} + x_5 \dot{x_5} + \varepsilon_1 \dot{\varepsilon_1} + \varepsilon_2 \dot{\varepsilon_2} + \varepsilon_3 \dot{\varepsilon_3} + \varepsilon_4 \dot{\varepsilon_4} + \varepsilon_5 \dot{\varepsilon_5} + \varepsilon_6 \dot{\varepsilon_6}).
$$

Taking the time derivative of the above function along the trajectories of (22), we have

$$
\dot{V} = -(k_1 x_1^2 + k_2 x_2^2 + k_3 x_3^2 + k_4 x_4^2 + k_5 x_5^2 + \eta \varepsilon_1^2 + \eta \varepsilon_2^2 + \eta \varepsilon_3^2 + \eta \varepsilon_4^2 + \eta \varepsilon_5^2 + \eta \varepsilon_6^2),
\tag{23}
$$

which is a negative function for $k_1, k_2, k_3, k_4, k_5 > 0$. Thus, due to the Lyapunov stability theory, we obtained that $\varepsilon_1(t) \to 0, \varepsilon_2(t) \to 0, \varepsilon_3(t) \to 0, \varepsilon_4(t) \to 0, \varepsilon_5(t) \to 0, \varepsilon_6(t) \to 0$ exponentially when $t \to \infty$.

4.1   Numerical simulation

Using the fourth-order Runge-Kutta method, we numerically simulate the adaptive control system introduced for system (16) with the adaptive control law (17) and the parameter update law (22). The parameters of system (2) are selected as $\alpha = 1.5, \sigma = 0.5, \beta = 30.9, \gamma = 3.5, \nu = 0.2, \xi = 0$. In addition, we take the adaptive and update laws as $k_i = \eta_i = 2$, where $i = 1, \ldots, 5$. Suppose that the initial values of the estimated parameters are $(0, 0, 0, 0, 0)$ and the initial values of system (2) are taken as $(1, 1, 1, 1, 1)$. When the adaptive control law (22) and the parameter update law (18) are used, the controlled system converges to equilibrium $E = (0, 0, 0, 0, 0)$ exponentially, as shown in Figure 9. The time responses of the error parameters are shown in Figures 10 - 15, while the time responses of the controlled system are displayed in Figures 16 - 20.
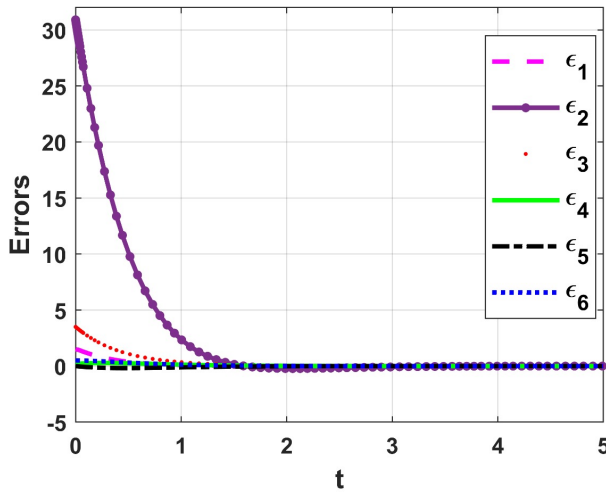
Figure 9: Time series of anti-synchronization for error dynamical system (22) with controller (17).
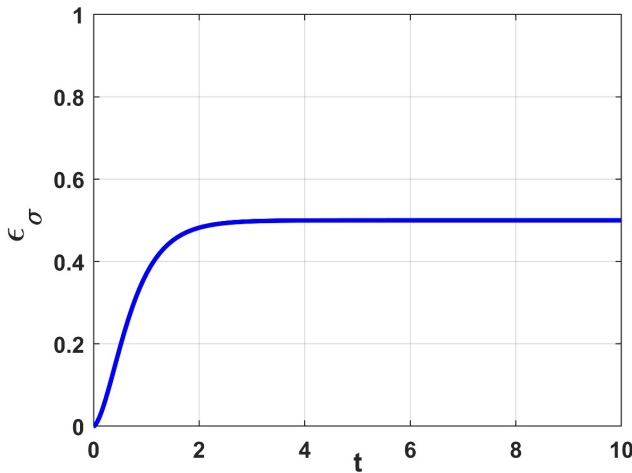

Figure 10: Time response of ε_σ.
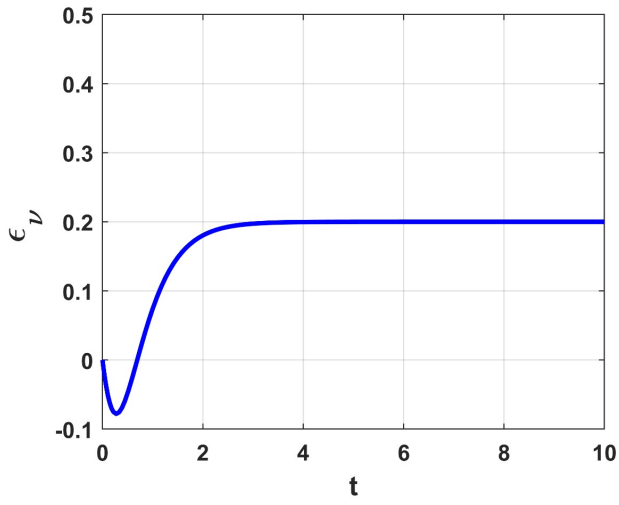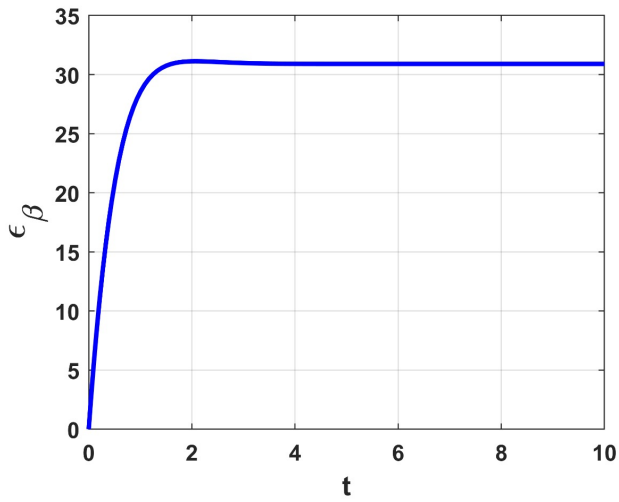
Figure 11: Time response of ε_ν.

Figure 12: Time response of ε_β.
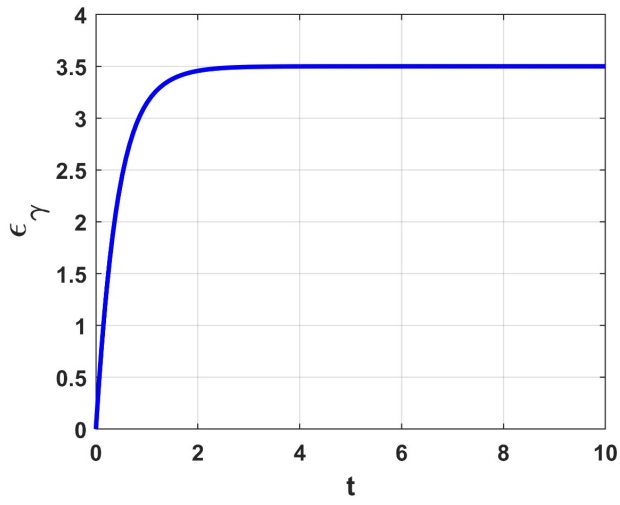
Figure 13: Time response of ε_γ.
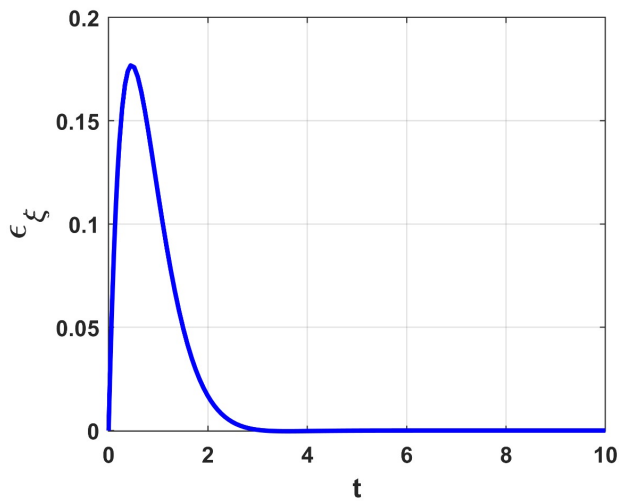
Figure 14: Time response of ε_ξ.

L. J. Sagban and A. A. Shukur

Malaysian J. Math. Sci. 18(3): 675–696 (2024) *675 - 696*
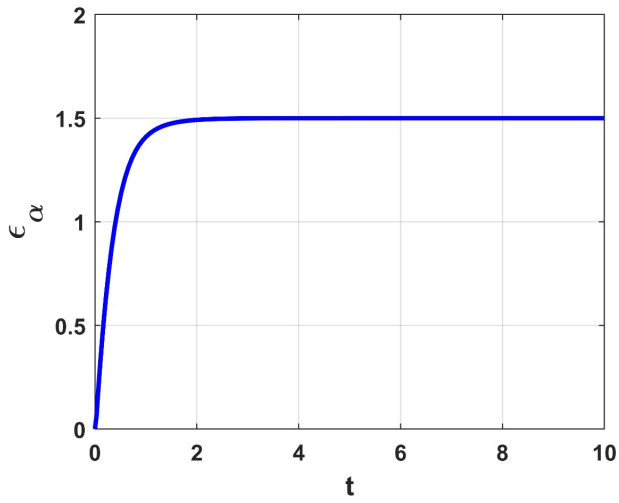
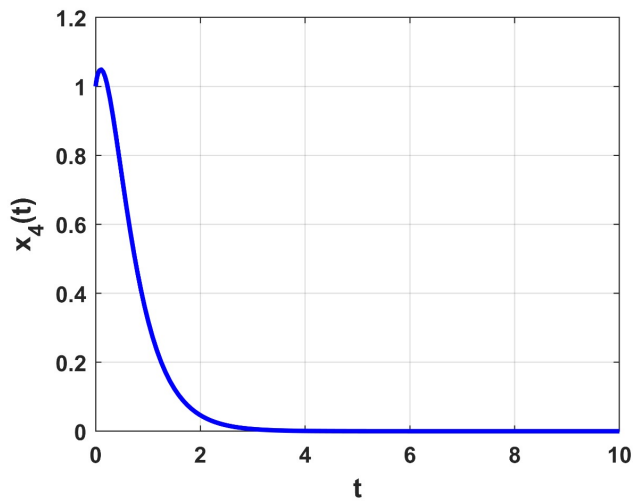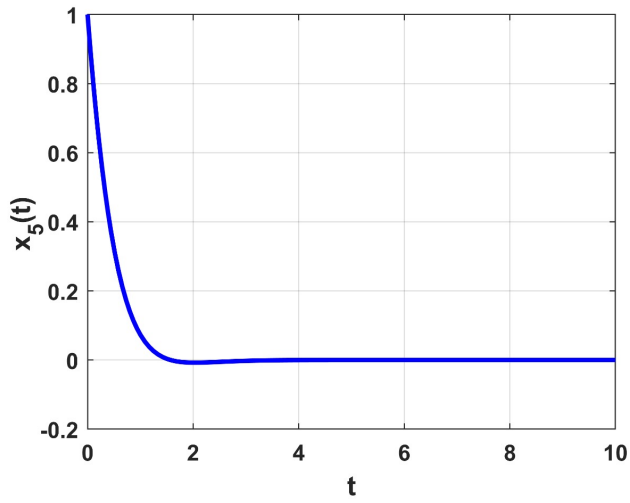Figure 15: Time response of ε_α.

Figure 16: Time response of $x_4(t)$.

Figure 17: Time response of $x_5(t)$.
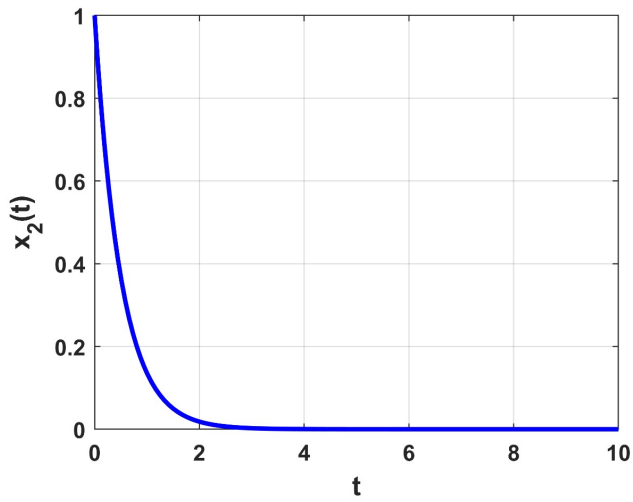
Figure 18: Time response of $x_2(t)$.

L. J. Sagban and A. A. Shukur

Malaysian J. Math. Sci. 18(3): 675–696 (2024) *675 - 696*
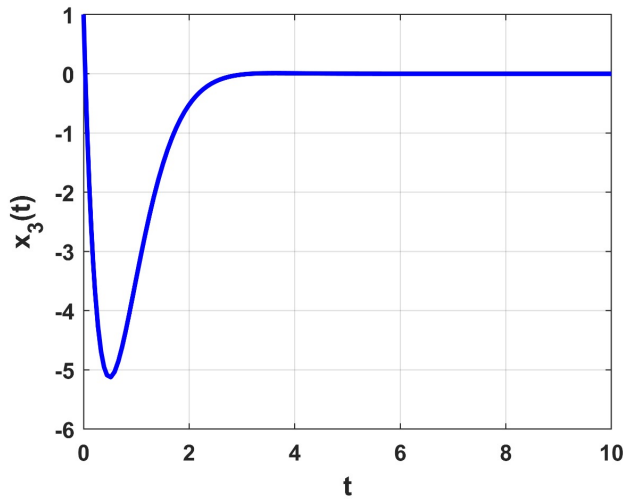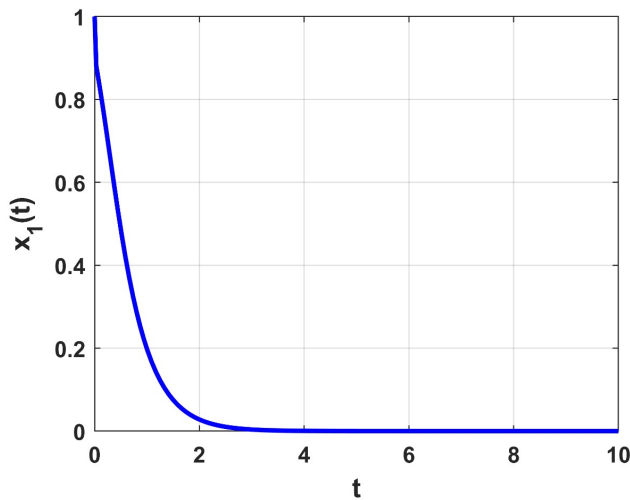
Figure 19: Time response of $x_3(t)$.

Figure 20: Time response of $x_1(t)$.

5 Conclusion

The complex dynamics of a novel five-dimensional hyperchaotic system involved with property that is uniformly measured system was investigated. Analyzing the proposed system shows that the proposed system can be classified either hidden attractor where no equilibrium appeared or self-excited with unusual nature of equilibrium points connected to Lambert W function appeared. In addition, we provided the adaptive control of the new system. In particular, the other dynamics of the introduced system of this paper are expected to be further studied.

Conflicts of Interest The authors declare no conflict of interest.

References

[1] S. F. Al-Azzawi & A. M. Hasan (2023). New 5D hyperchaotic system derived from the Sprott C system: Properties and anti synchronization. *Journal of Intelligent Systems and Control*, 2(2), 110–122. https://doi.org/10.56578/jisc020205.

[2] N. F. H. Al-Saffar, H. K. H. Alkhayyat & Z. K. Obaid (2024). A novel image encryption algorithm involving a logistic map and a self-invertible matrix. *Malaysian Journal of Mathematical Sciences*, 18(1), 107–126. https://doi.org/10.47836/mjms.18.1.07.

[3] E.-W. Bai & K. E. Lonngren (1997). Synchronization of two Lorenz systems using active control. *Chaos, Solitons & Fractals*, 8(1), 51–58. https://doi.org/10.1016/S0960-0779(96)00060-4.

[4] E.-W. Bai & K. E. Lonngren (2000). Sequential synchronization of two Lorenz systems using active control. *Chaos, Solitons & Fractals*, 11(7), 1041–1044. https://doi.org/10.1016/S0960-0779(98)00328-2.

[5] K. Benkouider, S. Vaidyanathan, A. Sambas, E. Tlelo-Cuautle, A. A. Abd El-Latif, B. Abd-El-Atty, C. F. Bermudez-Marquez, I. M. Sulaiman, A. M. Awwal & P. Kumam (2022). A new 5-D multistable hyperchaotic system with three positive Lyapunov exponents: Bifurcation analysis, circuit design, FPGA realization and image encryption. *IEEE Access*, 10, 90111–90132. https://doi.org/10.1109/ACCESS.2022.3197790.

[6] Y. Bian & W. Yu (2021). A secure communication method based on 6-D hyperchaos and circuit implementation. *Telecommunication Systems*, 77(4), 731–751. https://doi.org/10.1007/s11235-021-00790-1.

[7] R. M. Corless, G. H. Gonnet, D. E. G. Hare, D. J. Jeffrey & D. E. Knuth (1996). On the Lambert *W* function. *Advances in Computational Mathematics*, 5, 329–359. https://doi.org/10.1007/BF02124750.

[8] S. M. El-Shourbagy, N. A. Saeed, M. Kamel, K. R. Raslan, M. K. Aboudaif & J. Awrejcewicz (2021). Control performance, stability conditions, and bifurcation analysis of the twelve-pole active magnetic bearings system. *Applied Sciences*, 11(22), 10839. https://doi.org/10.3390/app112210839.

[9] S. Jafari & J. C. Sprott (2013). Simple chaotic flows with a line equilibrium. *Chaos, Solitons & Fractals*, 57, 79–84. https://doi.org/10.1016/j.chaos.2013.08.018.

[10] S. Jafari, J. C. Sprott, V.-T. Pham, C. Volos & C. Li (2016). Simple chaotic 3D flows with surfaces of equilibria. *Nonlinear Dynamics*, 86, 1349–1358. https://doi.org/10.1007/s11071-016-2968-x.

[11] N. A. Khan, M. A. Qureshi & N. A. Khan (2023). Evolving tangent hyperbolic memristor based 6D chaotic model with fractional order derivative: Analysis and applications. *Partial Differential Equations in Applied Mathematics*, 7, 100505. https://doi.org/10.1016/j.padiff.2023.100505.

[12] N. V. Kuznetsov, G. A. Leonov, M. V. Yuldashev & R. V. Yuldashev (2017). Hidden attractors in dynamical models of phase-locked loop circuits: Limitations of simulation in MATLAB and SPICE. *Communications in Nonlinear Science and Numerical Simulation*, 51, 39–49. https://doi.org/10.1016/j.cnsns.2017.03.010.

L. J. Sagban and A. A. Shukur

Malaysian J. Math. Sci. 18(3): 675–696 (2024) *675 - 696*

[13] E. N. Lorenz (2006). On the prevalence of aperiodicity in simple systems. In *Global Analysis: Proceedings of the Biennial Seminar of the Canadian Mathematical Congress, Calgary, Alberta, June 12–27, 1978*, pp. 53–75. Springer. https://doi.org/10.1007/BFb0069804.

[14] A. A. Neamah & A. A. Shukur (2023). A novel conservative chaotic system involved in hyperbolic functions and its application to design an efficient colour image encryption scheme. *Symmetry*, *15*(8), 1511. https://doi.org/10.3390/sym15081511.

[15] A. Nitaj (2017). Post quantum cryptography. *Malaysian Journal of Mathematical Sciences*, *11*(S), 1–28.

[16] Z. Peng, W. Yu, J. Wang, Z. Zhou, J. Chen & G. Zhong (2022). Secure communication based on microcontroller unit with a novel five-dimensional hyperchaotic system. *Arabian Journal for Science and Engineering*, *47*, 813–828. https://doi.org/10.1007/s13369-021-05450-9.

[17] J. H. Pérez-Cruz, E. A. Portilla-Flores, P. A. Niño-Suárez & R. Rivera-Blas (2017). Design of a nonlinear controller and its intelligent optimization for exponential synchronization of a new chaotic system. *Optik*, *130*, 201–212. https://doi.org/10.1016/j.ijleo.2016.10.140.

[18] O. E. Rossler (1979). An equation for hyperchaos. *Physics Letters A*, *71*(2-3), 155–157. https://doi.org/10.1016/0375-9601(79)90150-6.

[19] N. A. Saeed, H. A. Saleh, W. A. El-Ganaini, J. Awrejcewicz & H. A. Mahmoud (2024). An unusual chaotic system with pure quadratic nonlinearities: Analysis, control, and synchronization. *Chinese Journal of Physics*, *88*, 311–331. https://doi.org/10.1016/j.cjph.2023.12.038.

[20] A. Sambas, S. Vaidyanathan, X. Zhang, I. Koyuncu, T. Bonny, M. Tuna, M. Alçin, S. Zhang, I. M. Sulaiman, A. M. Awwal & P. Kumam (2022). A novel 3D chaotic system with line equilibrium: Multistability, integral sliding mode control, electronic circuit, FPGA implementation and its image encryption. *IEEE Access*, *10*, 68057–68074. https://doi.org/10.1109/ACCESS.2022.3181424.

[21] S. J. Schiff, K. Jerger, D. H. Duong, T. Chang, M. L. Spano & W. L. Ditto (1994). Controlling chaos in the brain. *Nature*, *370*(6491), 615–620. https://doi.org/10.1038/370615a0.

[22] A. A. Shukur, M. A. AlFallooji & V.-T. Pham (2024). Asymmetrical novel hyperchaotic system with two exponential functions and an application to image encryption. *Nonlinear Engineering*, *13*(1), 20220362. https://doi.org/10.1515/nleng-2022-0362.

[23] P. Sooraksa & G. Chen (2018). Chen system as a controlled weather model–physical principle, engineering design and real applications. *International Journal of Bifurcation and Chaos*, *28*(4), 1830009. https://doi.org/10.1142/S0218127418300094.

[24] J. C. Sprott (2020). Do we need more chaos examples? *Chaos Theory and Applications*, *2*(2), 49–51.

[25] R.-A. Tang, Y.-L. Liu & J.-K. Xue (2009). An extended active control for chaos synchronization. *Physics Letters A*, *373*(16), 1449–1454. https://doi.org/10.1016/j.physleta.2009.02.036.

[26] V. S. Udaltsov, J. P. Goedgebuer, L. Larger, J. B. Cuenot, P. Levy & W. T. Rhodes (2003). Communicating with hyperchaos: The dynamics of a DNLF emitter and recovery of transmitted information. *Optics and Spectroscopy*, *95*, 114–118. https://doi.org/10.1134/1.1595224.

[27] M. Varan & A. Akgul (2018). Control and synchronisation of a novel seven-dimensional hyperchaotic system with active control. *Pramana*, *90*(54), 1–8. https://doi.org/10.1007/s12043-018-1546-9.

L. J. Sagban and A. A. Shukur

Malaysian J. Math. Sci. 18(3): 675–696 (2024) *675 - 696*

[28] J. Wang, W. Yu, J. Wang, Y. Zhao, J. Zhang & D. Jiang (2019). A new six-dimensional hyperchaotic system and its secure communication circuit implementation. *International Journal of Circuit Theory and Applications*, *47*(5), 702–717. https://doi.org/10.1002/cta.2617.

[29] Z. Wang, Z. Xu, E. Mliki, A. Akgul, V.-T. Pham & S. Jafari (2017). A new chaotic attractor around a pre-located ring. *International Journal of Bifurcation and Chaos*, *27*(10), 1750152. https://doi.org/10.1142/S0218127417501528.

[30] Z. Wei & Q. Yang (2011). Dynamical analysis of a new autonomous 3-D chaotic system only with stable equilibria. *Nonlinear Analysis: Real World Applications*, *12*(1), 106–118. https://doi.org/10.1016/j.nonrwa.2010.05.038.

[31] C. Xiu, J. Fang & Y. Liu (2022). Design and circuit implementation of a novel 5D memristive CNN hyperchaotic system. *Chaos, Solitons & Fractals*, *158*, 112040. https://doi.org/10.1016/j.chaos.2022.112040.

[32] S. Yan, E. Wang, Q. Wang, X. Sun & Y. Ren (2021). Analysis, circuit implementation and synchronization control of a hyperchaotic system. *Physica Scripta*, *96*(12), 125257. https://doi.org/10.1088/1402-4896/ac379b.

[33] Q. Yang, Z. Wei & G. Chen (2010). An unusual 3D autonomous quadratic chaotic system with two stable node-foci. *International Journal of Bifurcation and Chaos*, *20*(4), 1061–1083. https://doi.org/10.1142/S0218127410026320.

[34] M. T. Yassen (2005). Chaos synchronization between two different chaotic systems using active control. *Chaos, Solitons & Fractals*, *23*(1), 131–140. https://doi.org/10.1016/j.chaos.2004.03.038.

[35] X. Zhu & W.-S. Du (2019). New chaotic systems with two closed curve equilibrium passing the same point: Chaotic behavior, bifurcations, and synchronization. *Symmetry*, *11*(8), 951. https://doi.org/10.3390/sym11080951.